Research Journal of Environmental Sciences

ISSN 1819-3412

Academic
Journals Inc.

www.academicjournals.com

Research Journal of Environmental Sciences 9 (3): 137-151, 2015
ISSN 1819-3412 / DOI: 10.3923/rjes.2015.137.151

Optimum ARX Model Prediction for Monthly Air Temperature Changes in Delta, Egypt

[1]Mosbeh R. Kaloop, [2]Mohamed M. Abdelaal and [3]H.T. El Shambaky
[1]Department of Public Works Engineering, Faculty of Engineering, Mansoura University, 35516, Egypt
[2]Department of Geography, Faculty of Education, Mansoura University, 35516, Egypt
[3]Department of Civil Engineering, Misr Higher Institute for Engineering and Technology, Mansoura, Egypt

Corresponding Author: Mosbeh R. Kaloop, Department of Public Works Engineering, Faculty of Engineering, Mansoura University, 35516, Egypt

ABSTRACT

This study aims to study the ability application of nonlinear Auto-Regression model with exogeneous inputs (ARX) in forecasting time series monthly temperatures changes in Delta, Egypt for 49 years (1960 to 2009) monitoring data. Three methods are used to estimate the optimal parameters of ARX model identification which are the normalized Least Mean Square (LMS), artificial Neural Network (NN) and Wavenet Neural network (WN). The time series temperature changes from 18 weather stations in Delta are used to compare and estimate the best method for the temperature change models. The models results indicate that the worst case solution for ARX model is LMS while the WN is found to be better than NN in the training period. The NN is found an acceptable performance for training and testing periods. The 95% auto-correlation function for the residuals models shows that there is no loss of information is observed for the applied ARXNN model; however, the ARXNN technique can be successfully used to predict the monthly temperatures of any site at the Delta area in Egypt.

Key words: Temperature, ARX, least mean square, neural network, wavenet, delta, Egypt

INTRODUCTION

The global temperature changes are one of main aims of studies for the climate changes in recent years (Molua *et al*., 2010; NOAA., 2015; NASA., 2015). It is known that the temperature changes are affected on the land and sea areas. In addition, the temperature used as input parameters to estimate the climate changes or effectiveness of climate change parameters for the prediction modeling (Mpelasoka *et al*., 2001; Kisi and Shiri, 2014; Kisi and Sanikhani, 2015). The climate studies, especially climate change studies, argue that data sets should be based on homogeneity-adjusted data because the original time series could give a misleading description of the evolution of climate (Tuomenvirta, 2001). The long-term changes are observed to investigate the real causative factors which are usually small and slow and are often masked by large year-to-year variability (Raino, 1999). Moreover, most long-term series have been affected by many non-climatic factors leading to heterogeneity, including alterations of observatory location, surrounding environments, instruments, formulae used to calculate means, observing practices, observers, etc. (Li *et al*., 2004; Vicente-Serrano *et al*., 2010).

The used area in Egypt is divided into two important areas which are Nile Delta and Valley. These areas contain the main activity of peoples and high-density population. In the Nile Delta area, the air temperature changes are a great importance for irrigation scheduling and hydrological management as well as for soil and plant-related studies and agro-hydrologic fields (Domroes and El-Tantawi, 2005; Molua *et al*., 2010; Abdelaal, 2014). In addition, the Nile Delta is the richest farmland in Egypt; it also contains the largest cities after Cairo, which are Alexandria, Tanta, Damanhur, Mansoura and Zagazig. About half of Egypt's 90 million people live in the Delta region. The average population density in the Egyptian Delta is 1,500 persons km^{-2} or more (CAPMS., 2014). Therefore, The Delta is among the most densely populated agricultural areas in the world. Also in the Nile Delta, urban sprawl and Stalinization are the dominant degradation process. Moreover, the shoreline change is affected during last year because of the sea level change, which is affected due to world temperature change (Frihy and Komar, 1993; Ghoneim *et al*., 2015). For these reasons, the importance of temperature predictions has been increased over this area.

The prediction models for temperature air change are good tools to evaluate the land characterizing a change and hydrological changes (Kisi and Shiri, 2014; Kisi and Sanikhani, 2015). However, many numbers of studies have been carried out to model air temperature variations which need to estimate the high accurate nonlinearity temperature change effect estimation. The input parameter for the models used different in-between some studies. For examples, Kisi and Shiri (2014) have used the number of the months, station latitude, longitude and altitude values as input parameters to predict the monthly temperature change values and the used models are Adaptive Neuro-Fuzzy Inference System (ANFIS) and artificial Neural Networks (NN). The results for this study found that the NN was better than ANFIS model. Sargazi *et al*. (2014) have applied regression polynomial and NN to predict the model in Iran based on time series temperature monitoring stations and the results have shown that the NN is better and can be used to predict the temperature change. Kisi *et al*. (2013) have used two different NN models, Generalized Regression Neural Networks Model (GRNNM) and Kohonen Self-Organizing Feature Maps neural networks model (KSOFM) and two different ANFIS models, ANFIS model with sub-clustering identification (ANFIS-SC) and ANFIS model with grid partitioning identification (ANFIS-GP), for estimating daily dew point temperature. The climatic data that consisted of 8 years of daily records of air temperature, sunshine hours, wind speed, saturation vapor pressure, relative humidity and dew point temperature from three weather stations in South Korea were used in the study. The estimated models of this study show that the ANFIS-SC, ANFIS-GP and GRNNM models reveals a good accuracy that can be used to predict the dew point temperature. Moreover, other studies of models can be seen in (Sinik, 1992; Baigorria *et al*., 2004; Kisi and Sanikhani, 2015).

In Egypt, the air temperature prediction models are limited and used traditionally prediction models (El-Hussainy and Essa, 1997; Omran, 2000; Domroes and El-Tantawi, 2005; El Kenawy *et al*., 2010; Abdelaal, 2012). However, the main aim of this study is to use the auto-regression model with eXogeneous inputs model identification with different solutions (least Mean Square, neural network and wavelet neural network) to estimate and predict the air temperature changes. The 49 years' time series monitoring 18 stations are used to estimate a best model that can be used in the Nile Delta region.

STUDY AREA AND MEASUREMENTS

Egypt lies in the northeastern corner of the African continent. It extends between 22 and 32°N, 25 and 37°E with an overall area of approximately 1,019,600 km^2, about 93% of this area is desert.

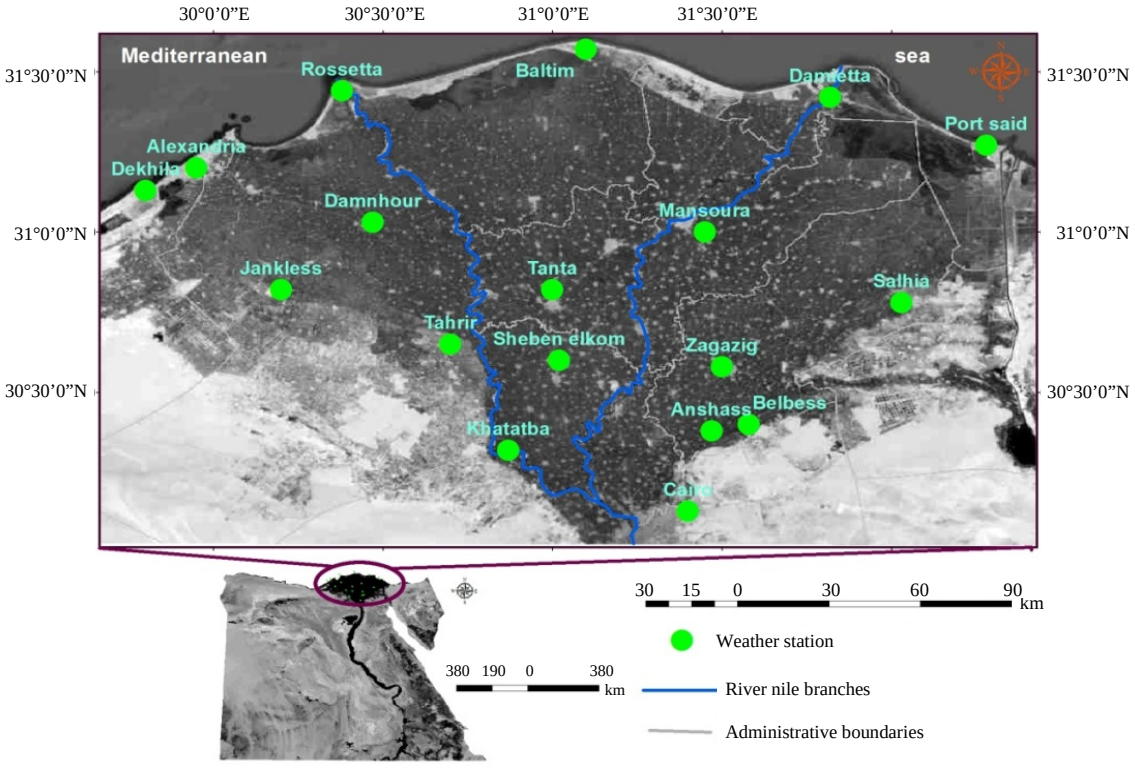

Fig. 1: Point monitoring distribution and positions

Egypt's heartland lies in the Nile Delta in the north or Lower Egypt. This is, where the bulk of the country's industries, agriculture and population are located. The rest of the country is predominantly deserted.

The Nile delta is located in Northern Egypt, begins north of Cairo, where the Nile spreads out and drains into the Mediterranean Sea, as shown in Fig. 1. The two main river branches spread out in a V-shaped fan and make their way towards the Mediterranean through delta, the Damietta in the east and the Rosetta in the west, from south-to-north, the delta is approximately 160 km's in length. From west-to-east, it covers some 240 km of Mediterranean coastline. Delta covers an area of 22,000 km², represented about 2.2% of the total area of Egypt. The Delta extends as administrative area to include 12 governorates. It extends between 29°45' and 31°30'N and 29°22' and 32°20'E.

The Delta has a hot arid climate (Köppen: BWh) as the rest of Egypt, but its northern most part, as is the case with the rest of the northern coast of Egypt (Köppen: CSb), which is the wettest region in the country, where the average annual rainfall is more than 100 mm. It has relatively moderate temperatures, with mean maximum temperature usually not surpassing 31°C in the summer. The delta characterized by little winter rainfall, with an annual average about 25 mm, most of this falls in the winter months. July and August are hottest months in Delta, with mean maximum temperature 35°C. Winter mean minimum temperatures are normally in the range of 5°C at nights to 17°C at days. In this study, monthly observed data are collected from 18 spatially-representative observatories in Egyptian delta during the period 1960-2009.

Table 1: Summary measurement studied weather stations

Station	Geographical coordinates		Altitude (m) above M.S.L	Mean temperature	
	Latitude	Longitude		Max (°C)	Min (°C)
Dekhila	31°8	29°48	2.53	24.40	16.42
Alexandria	31°12	29°57	-3.53	24.62	15.57
Rossetta	31°23	30°24	1.70	24.99	15.89
Baltim	31°33	31°6	1.00	24.47	15.54
Damietta	31°25	31°49	1.98	24.47	15.26
Port Said	31°16	32°17	0.80	24.33	18.28
Salhia	30°47	32°°2	6.50	27.47	14.15
Mansoura	31°0	31°27	3.75	27.58	13.51
Damanhour	31°2	30°28	3.47	27.10	14.68
Janaklees	30°49	30°12	9.50	26.85	14.87
Tahrir	30°39	30°42	16.00	28.20	14.11
Shebinelkom	30°36	31°1	11.50	28.23	13.94
Tanta	30°49	31°0	8.35	27.16	14.40
Khatatba	30°19	30°52	15.20	27.90	14.19
Anshass	30°23	31°28	29.77	27.68	15.49
Belbaiss	30°24	31°35	29.48	27.83	15.39
Zagazig	30°35	31°30	8.00	28.41	15.97
Cairo	30°8	31°24	64.12	28.33	15.98

The data were obtained from the Egyptian Meteorological Authority (EMA). A list of observatories and their coordinates are shown in Table 1 and Fig. 1. In order to examine data quality, such data underwent some quality control and homogenization procedures recommended by the World Meteorological Organization (WMO) (WMO/TD., 2003). The quality of measurement control is a fundamental task to ensure the quality of climatic data before performing climatic analyses, such as long-term climatic change and variability and to assess climate related issues (WMO/TD., 2003; Kenawy *et al*., 2010). The objective of quality control is to identify erroneous or questionable records in the climate datasets (Vicente-Serrano *et al*., 2010). Traditionally, quality control is the easiest and most common technique to test the data for outliers (Peterson *et al*., 1998).

The reconstruction and gap filling of spatially-close data series is an urgent demand to build serially-complete datasets and to generate new and unique series using reference series depending on their composition on neighboring observatories to the candidate observatory (Peterson and Easterling, 1994; Vicente-Serrano *et al*., 2010). A homogenization technique was employed based on "Standard Normal Homogeneity Test" (SNHT), developed by Alexandersson (1986), for a single break being the most widely used, in addition to reference series (Peterson and Easterling, 1994). The AnClim software developed by Stepanek (2007) was used to carry out SNHT. For more details, Kenawy *et al*. (2010) and El Kenawy *et al*. (2010) are concluded, the quality control for the air temperature stations used in this study.

METHODOLOGY RESULTS AND DISCUSSION

Pre-analysis temperature data: Table 1 shows the mean temperature for the area monitoring measurements. From this table, it can be seen that the temperature increases with moving to the south direction. Moreover, it can be seen that the mean maximum average temperature in summer in between 24.40 and 28.41°C while in the winter time in between 13.51 and 18.28°C. However, the near stations to the sea area are shown lower temperature in summer. Figure 2 show the 600 months monitoring time series for the selected points, Port said (Pors) and Dekhila (Dekh) are selected as a near to the sea area. Mansoura (Mans) as a mid-study area and Khatatba (Khat) and Anshass (Ans) as a southern study area and far from sea effect. From this figure, it can be seen that

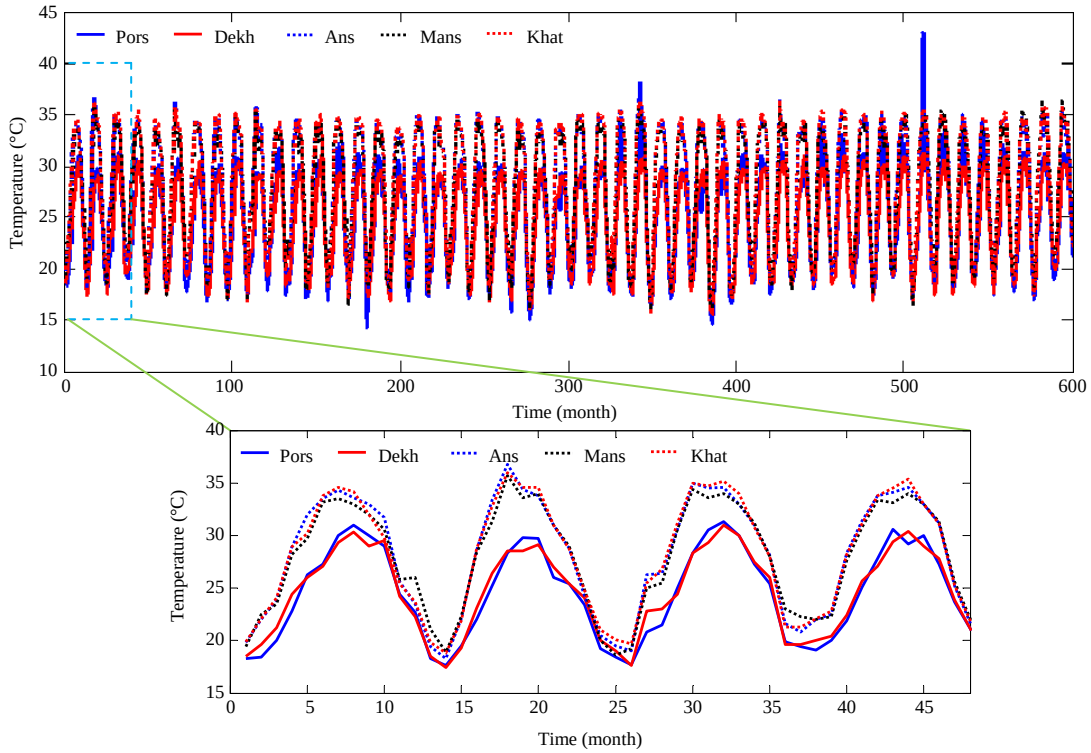

Fig. 2: Time series temperature change for 49 years

Table 2: Linear fit regression for time series monitoring points

Station	Linear fit Eq.	Station	Linear fit Eq.
Port Said	y = 1.9e-3x+24	Tanta	y = 1.5e-4x+27
Damietta	y = 1.1e-3x+24	Salhia	y = 1.4e-4x+27
Baltim	y = 1.3e-3x+24	Tahrir	y = 3.3e-4x+28
Rosetta	y = 1.4e-3x+25	Shebinelkom	y = 3.8e-4x+28
Alexandria	y = 1.5e-3x+24	Zagazig	y = 7.1e-4x+28
Dekhaila	y = 1.1e-3x+24	Belbaiss	y = 4.5e-5x+28
Damanhour	y = 7.5e-4x+27	Anshass	y = 2.1e-5x+28
Mansoura	y = 7.1e-4x+27	khatatba	y = 3.4e-4x+28
Janaklees	y = 6.3e-4x+27	Cairo	y = 6.5e-4x+28

*y is temperature and x is time in months

the correlation between Port Said and Dekhila points is high and the correlation between Khatatba, Anshass and Mansoura is high. In addition, it can be seen that the maximum variance is occurred in the summer time, while low variance occurs during winter time. However, the summer time temperature change is higher than winter time.

The linear fit regression for monitoring time series temperature observations are shown in Table 2. From this table, it can be seen that the coast points are higher temperature changes than that other points. Moreover, it can be seen that the slope temperature change is decreased at points far from the coastal line. However, in Delta the main change in temperature is occurred at the coastal points monitoring.

ARX model identification and solution models: The nonlinear auto-regression model with eXogeneous inputs (ARX) identification model is used in this study to estimate the prediction model

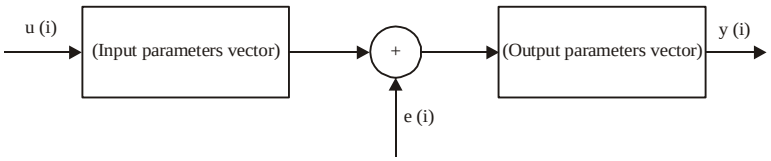

Fig. 3: ARX diagram model

Table 3: Summary statistical training points

	ARX		ARXNN		ARXWN	
Stations	RMSE (°C)	R	RMSE (°C)	R	RMSE (°C)	R
Port said	3.940	0.599	0.608	0.992	3.63e-14	0.999
Baltim	1.810	0.933	0.849	0.982	4.39e-14	0.999
Alexandria	1.550	0.943	0.968	0.977	4.20e-14	0.999
Damnhour	2.030	0.923	1.121	0.977	2.36e-14	0.999
Salhia	1.650	0.956	0.977	0.985	2.96e-14	0.999
Tanta	2.448	0.902	1.527	0.963	2.22e-14	0.999
Shebenelkom	2.069	0.940	0.901	0.989	1.85e-14	0.999
Anshass	1.855	0.947	0.711	0.992	2.62e-14	0.999
Cairo	2.090	0.941	1.144	0.983	1.83e-14	0.999

can be used to detect the temperature change in Delta. The ARX model is a time series model depend on the past time series, current with past values of driving values and model errors (Kaloop *et al*., 2014). The input-output ARX model of order [na nb] can be expressed as follow:

$$y_i+a_1y_{i-1}+a_2y_{i-2}+\cdots+a_{na}y_{i-na} = b_1u_{i-1}+b_2u_{i-2}+\cdots+b_{nb}u_{i-nb}+e_i \quad (1)$$

where, is the estimated output at time i, are previous system states (y) and are input (u) observations and are the ARX model parameters for past output order (na) and past input order (nb), respectively and e is the error or noise term. The general input-output model structure used for modeling of nonlinear temperature change with constant time invariant excited by deterministic input is shown in Fig. 3. Assuming unit sampling interval is a monthly interval and the input-output quantity u(i) and y(i), respectively, are selected based on time history monitoring and geographical position point distributions to cover the whole study area.

To estimate the parameters and predict the ARX model identification, three methods are used in this study which are Least Mean Square (LMS), artificial Neural Network (NN) and wavelet neural network methods (wavenet); the following sections concluded description the methods used. In this study the time series monthly averaged temperature values at 18 weather stations in Delta, Egypt, by ARX model are used. In this way, selected training and testing point's randomly. The points in Table 3 and 4 are used as training and testing, respectively. The selected training and testing points are covered the whole area of Delta. The system of multi-input multi-output is used in this model. Before applying the ARX models to the data, training input and output values were normalized using the following equation:

$$T = \frac{T_0 - T_m}{\sigma T} \quad (2)$$

where, T_0, T_m and σ_T are observation, mean and standard deviation of monitoring temperature, respectively. The results re-normalized to original observation to compare results and estimated the best prediction solution.

Table 4: Summary statistical testing points

	ARX		ARXNN		ARXWN	
Stations	RMSE (°C)	R	RMSE (°C)	R	RMSE (°C)	R
Damietta	3.869	0.604	0.923	0.980	1.037	0.977
Rossetta	1.970	0.920	0.670	0.989	0.949	0.979
Dekhila	1.382	0.950	0.817	0.982	0.738	0.992
Mansoura	2.087	0.928	1.003	0.984	1.070	0.988
Jankless	1.624	0.951	1.008	0.981	0.925	0.991
Tahrir	1.916	0.940	0.979	0.985	1.431	0.981
Belbess	1.961	0.941	1.204	0.978	1.055	0.986
Khatatba	1.761	0.952	0.941	0.987	0.624	0.996
Zagazig	2.703	0.893	1.063	0.984	2.077	0.938

Three statistical indices are used to evaluate the models; First, correlation coefficient of determination (R) defined as in Eq. 3 and ranged between 0 and 1; the higher the value of R, the better quality of the model:

$$R = \frac{\sum_{i=1}^{n}(T_1 - \overline{T}_t)(T_t^p - \overline{T}_t^p)}{\sqrt{\sum_{i=1}^{n}(T_1 - \overline{T}_t)^2 \sum_{i=1}^{n}(T_t^p - \overline{T}_t^p)^2}} \quad (3)$$

where, T_t and T_t^p are observed and predicted temperature change at time t = 1,….n, respectively. Second, Root Mean Square Error (RMSE) defined as in Eq. 4 and smaller value of RMSE means better quality of the model:

$$RMSE = \sqrt{\frac{1}{n}\sum_{i=1}^{n}(T_t - T_t^p)^2} \quad (4)$$

The third performance criterion for a model is provided by the Auto-Correlation Function (ACF) of the residuals $(e_t = T_t - T_t^p)$. The lag (m) Auto-Correlation (AC) is defined as in Eq. 5:

$$\lambda(m) = \frac{1}{n}\sum_{t=1}^{n} e_t - m^e t \quad (5)$$

The AC λ(m) is zero, when parameter model (k) is nonzero. A large AC, when k is nonzero indicates that the residual is not zero-mean error and also implies that the model structure is not relevant to the system or that there might be a need to increase the model order. In real world applications, AC λ(m) cannot be zero, when m is nonzero because of limited length of observation points. If the value of AC falls within 95% of the confidence interval, the AC value is insignificant and this value is considered to be equal to zero.

Least mean square: In this method assuming that the prediction estimated output, input-output vector φ_i and unknown parameters θ as follow:

$$y = \varphi\theta + e \quad (6)$$

where, $\varphi = [-y_{i-1}-y_{i-2}\ldots u_{i-1}u_{i-2}\ldots]^T$; $\theta = [a_1\ a_2\ldots b_1\ b_2\ldots]$ and using normal least square method to estimate the unknown parameters as follow:

$$\theta = (\varphi^T\varphi)^{-}1\ \varphi^T y \tag{7}$$

$$\nu = y\text{-}\varphi\theta \tag{8}$$

where, ν is the vector of the n residuals, the residuals can be used to correct the prediction results. The e vector is used a random vector error with E(e) = 0; Var(e) = σ^2.

In this section, the ARX model is used with order number of input and output data [na = 9, nb = 9] and one delay for the input time series (ARX order [9 9]). The LMS (Eq. 6-8) is used to estimate the parameters and calculated the identification results as shown in Table 3 and 4. In addition, Fig. 4 illustrates the selected prediction for the Port Said, Mansoura and Khatatba points and auto-correlation error test. From Table 3, it can be seen that the RMSE and R range are1.55-3.94°C, 0.599-0.956 for testing points and 1.382-3.869°C and 0.604-0.951 for training points, respectively. From Fig. 4, it can be seen that the auto-correlation model residuals are not in 95% confidence intervals for the testing and training point's selection. However, it can be concluded that the loss of information was observed since the residuals of this model not stayed within the confidence interval of the auto-correlation function. From these results, it can be concluded that the least square solution cannot be confident to predict the temperature change in the Nile Delta.

Artificial neural network: A multilayer Neural Network has been used in this section. It has three layers including input (n1), hidden (n2) and output (n3) layers as shown in Fig. 5. According to the complexity of the problems, the number of hidden layers may increase. When the input layer receives information at each node, the information is weighted and transferred to the nodes of the hidden layer. The hidden layer also transfers the information to the output layer. Then, the output of the neural network is obtained. The number of layers and that of nodes in each layer should be chosen by experiences or trial and errors. This strategy has been well described in the referenced papers (Kim and Lee, 2001), thus just a summary is provided in this section. The hidden layer outputs are stated as below.

The inputs to the network are denoted by z_{n1} and the net outputs of the activation function of the hidden layer (f^1) hidden layer are expressed as follows:

$$O_i^1 = f^1\left(\sum_{k=1}^{n1} W_{ik}^1 Z_k + b_i^1\right)\ (i = 1, 2,...n2) \tag{9}$$

where, W_{ik}^1 is the connection weight between the input and b_i^1 hidden layers and the bias of the hidden layer. Likewise, the relationship between the net hidden and output of the second layer is:

$$O_i^2 = f^2\left(\sum_{i=1}^{n1} W_{ji}^2 O_i^1 + b_i^2\right)\ (i = 1, 2,...n3) \tag{10}$$

where, W_{ji}^2 is the connection weight between the hidden and output layers and b_i^2 the bias of the output layer.

The weights and biases should be determined in order that the neural network predicts the desired output. The determination of the optimal weights and biases is the so-called learning or training. Training is accomplished by minimizing a criterion defined by the squared sum of the

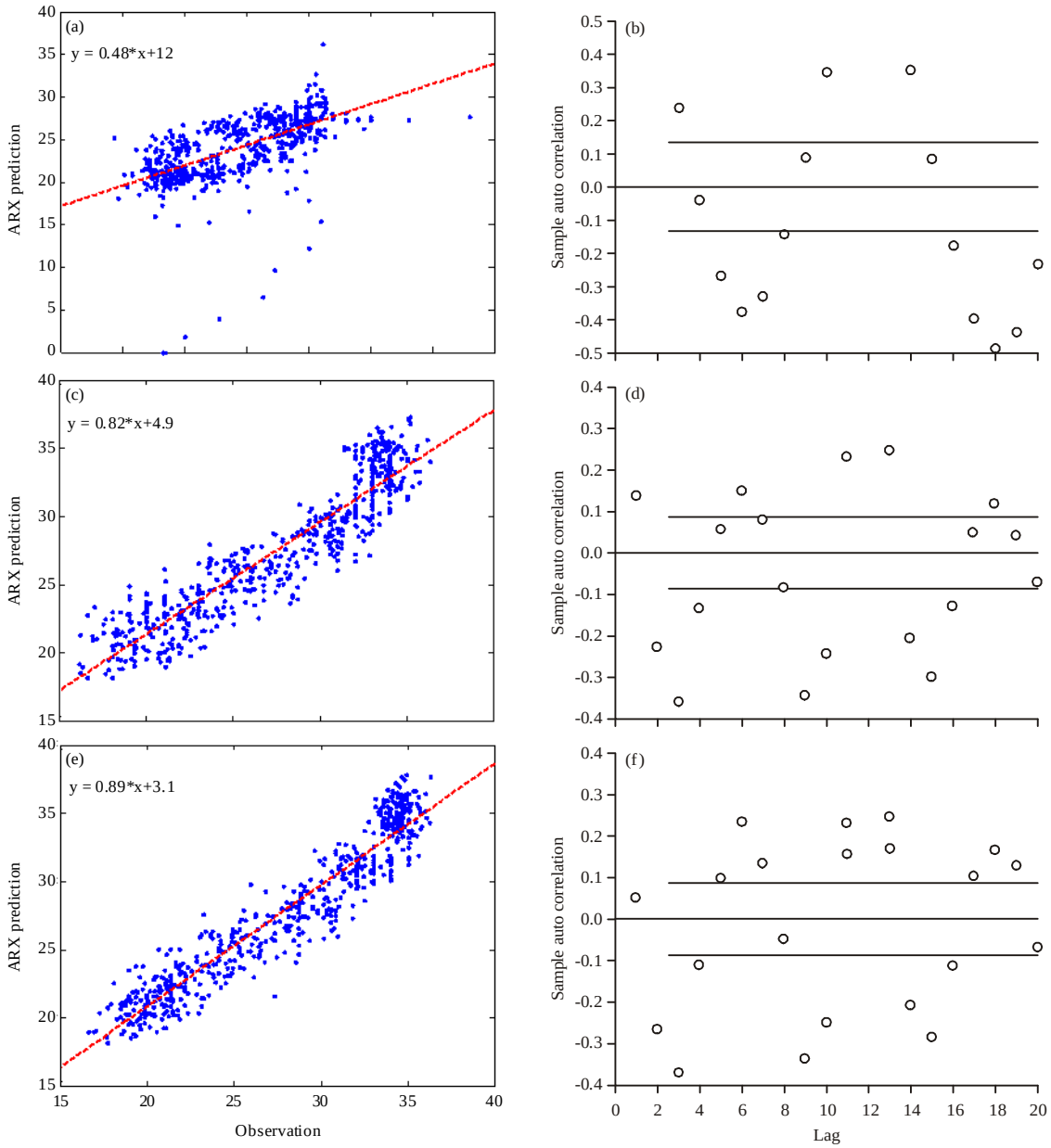

Fig. 4(a-f): ARX model with LMS prediction and ACF confidence, (a) Port said prediction, (b) Port said ACF and 95% confidence, (c) Mansoura prediction, (d) Mansoura ACF and 95% confidence, (e) Khatatba prediction and (f) Khatatba ACF and 95% confidence

offset values between the actual and the desired outputs of the neural network (Kim and Lee, 2001). By minimizing the error function through training rule, the network outputs become close to the desired outputs. Finally, when the neural network receives input, it predicts the desired output.

In this study, the series-parallel nonlinear ARXNN is used to identify the temperature model prediction. A difficult task with NN involves choosing the hidden nodes number. Here, the NN with

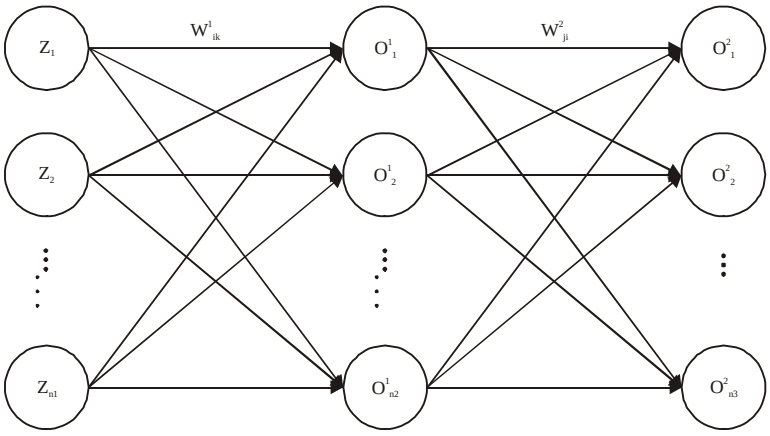

Fig. 5: Structure of one hidden layer multilayer perceptron

one hidden layer was used and the hidden nodes number was determined using trial and error method. The tangent sigmoid activation function was used for the hidden and output nodes (Eq. 9 and 10). The NN network training was stopped after 500 epochs since the variation of error was too small after this epoch. The number of input and output are the number of training and testing points as shown in Table 3 and 4 (ARXNN order [9 9]). The results of this method are shown in Table 3, 4 and Fig. 6. Figure 6 shows that the ACF and identification results for Port Said, Mansoura and Khatatba points. From Table 3, it can be seen that the training statistical results referred that the RMSE for ARXNN between (0.608-1.527°C) and R between (0.963-0.992). Moreover, Table 4 illustrates that the testing point statistical ARXNN results. From Table 4, it can be seen that the RMSE range is (0.670-1.204°C) and R range is (0.978-0.989). Moreover, it can be seen that ACF for selection points within 95% confidence intervals for the testing and training; however, no loss of information was observed since the residuals of this model stayed within the confidence interval of the auto-correlation function. From the results, it can be concluded that the NN solution is better than LMS solution. Moreover, the results show that the ARXNN model can be used to predict the temperature of the Nile Delta region.

Wavelet neural network: The same for previous NN system the multilayer Neural Network has been used in this part. It has three layers including input (n1),wavelet (n2) and output (n3) layers as shown in Fig. 5 with wavelet layer replaced for hidden layer. The process of wavenet method is the same for the NN with relationship between the net input and output of the second layer as follow:

For the input signal sequence z_{n1}, the output of the wavelet layer is calculated as:

$$O_j^1 = \varphi_j\left[\frac{\sum_{i=1}^{n1} w_{ij} Z_i - b_i}{a_j}\right],\ j = 1, 2, ,..., n2 \tag{11}$$

where, O_j^1 is the output value for the node j in the wavelet layer, the wavelet functions φ_j; all lying on the same layer are called wavelet wavelons. The choice of the wavelet function depends on the specific application . There are many wavelet function can be used. In this study used Mexican hat

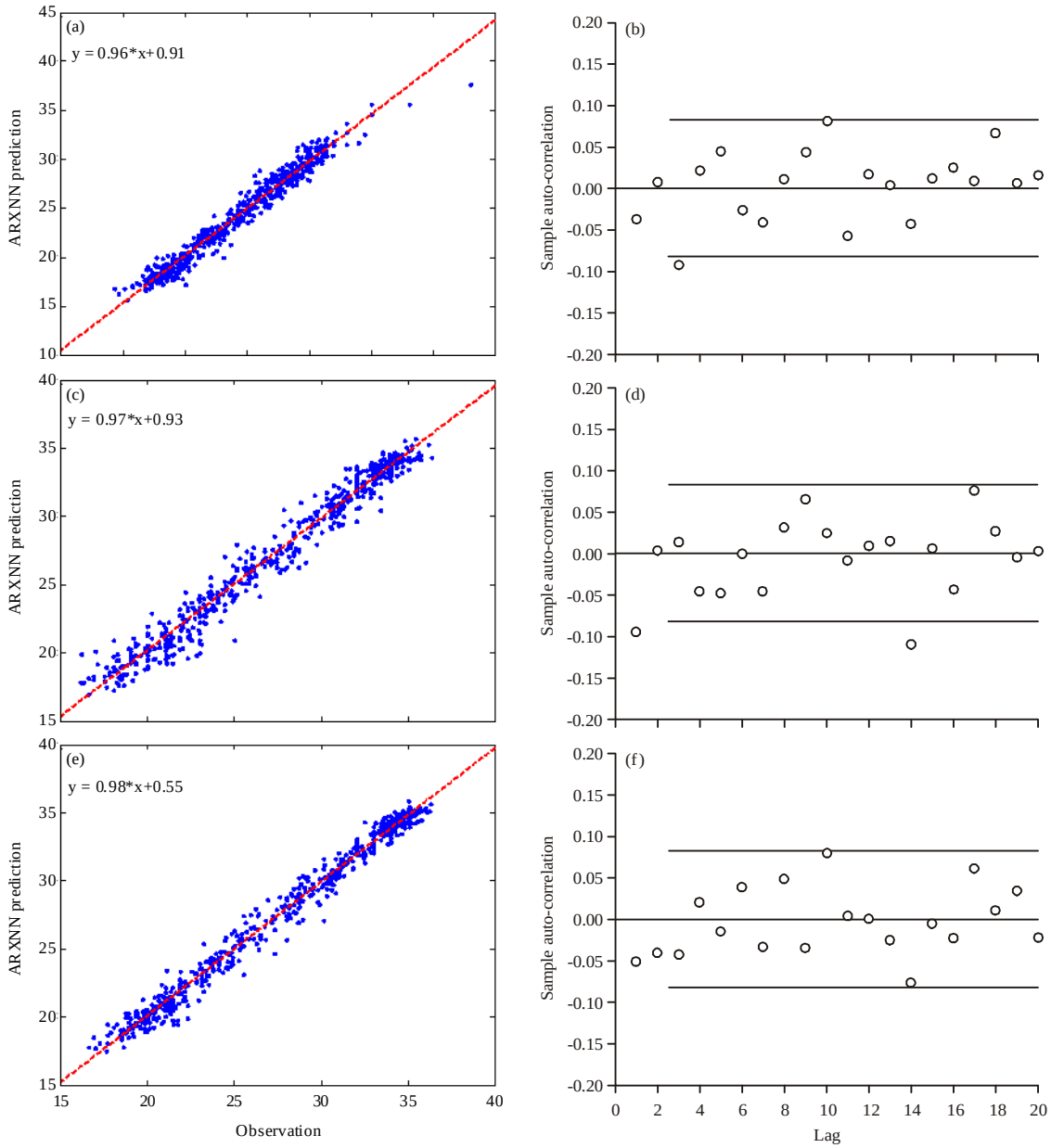

Fig. 6(a-f): ARXNN model prediction and ACF confidence, (a) Port said prediction, (b) Port said ACF and 95% confidence, (c) Mansoura prediction, (d) Mansoura ACF and 95% confidence, (e) Khatatba prediction and (f) Khatatba ACF and 95% confidence

function to implement the proposed nonlinear temperature changes model and used a linear functions output (f); w_{ij} is the weight connecting the input layer and wavelet layer; bj is the bias of the hidden layer and aj is the stretch factor of φ_j. However; the output layer can be calculated as:

$$Q_t^2 = f\left(\sum_{i=1}^{n3} W_{it} O_i^1\right),\ t = 1, 2, ..., n3 \tag{12}$$

where, w_{it} is weight connecting the wavelet layer and output.

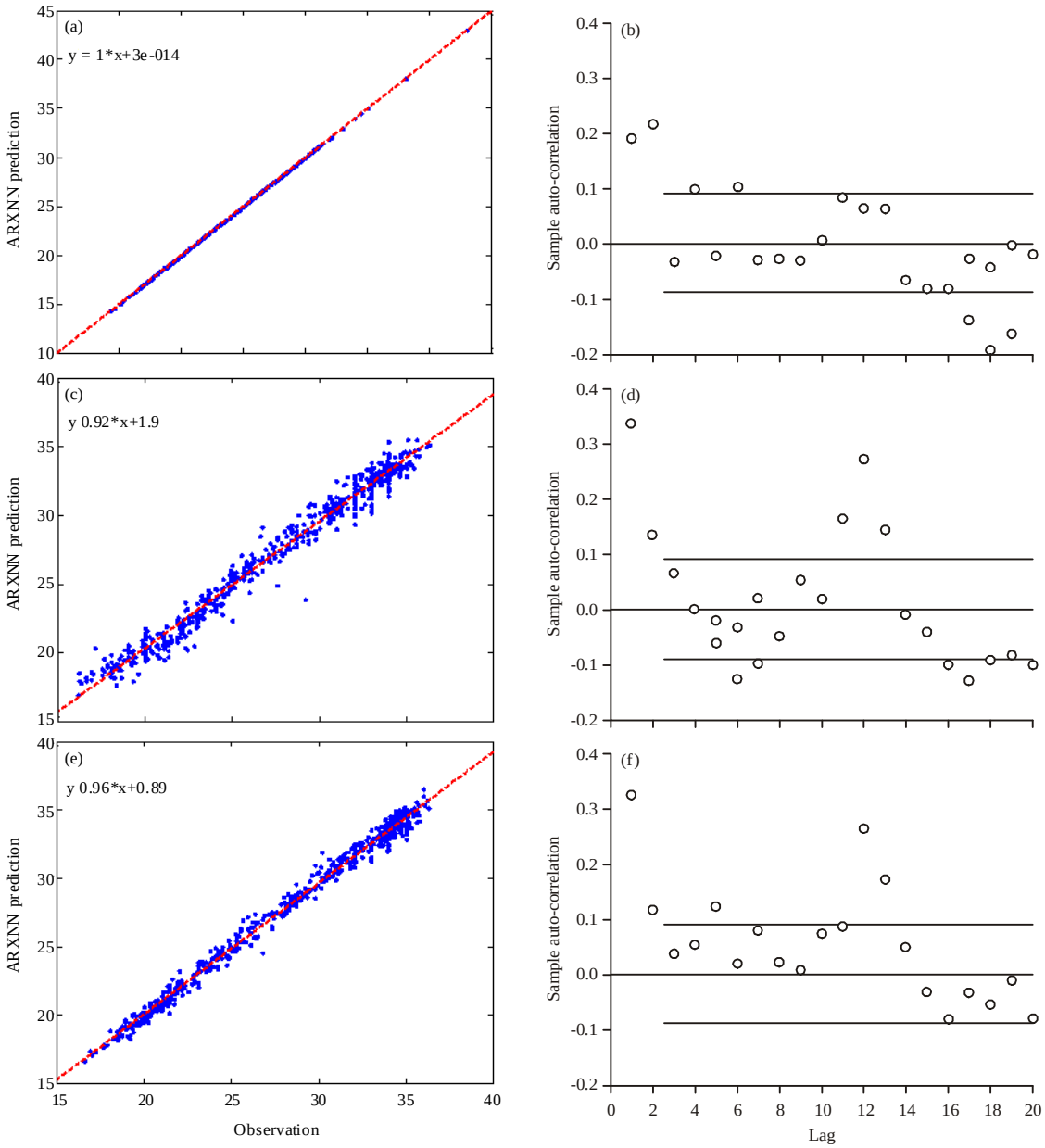

Fig. 7(a-f): ARXWN model prediction and ACF confidence, (a) Port said prediction, (b) Port said ACF and 95% confidence, (c) Mansoura prediction, (d) Mansoura ACF and 95% confidence, (e) Khatatba prediction and (f) Khatatba ACF and 95% confidence

In this section, the nonlinear ARX Wavelet Neural network (ARXWN) is used to identify the temperature model prediction. As the same as previous, the WNN with one wavelet layer was used and the wavelet nodes number was determined using trial and error method. The wavelet with 100 nodes was used for the wavelet layer. The number of input and output are the number of training and testing points as shown in Table 3 and 4 (ARXWN order [99]). The results of this method are shown in Table 3 and 4 and Fig. 7. Where, Fig. 7 shows that the ACF and identification results for Port Said, Mansoura and Khatatba points.

From Table 3, it can be seen that the training statistical results referred that the RMSE for ARXWN near to 0°C and R is 0.99 for all training points. Moreover, Table 4 shows that the testing point statistical ARXWN results. From this Table 3, it can be seen that the RMSE range is (0.624-2.077°C) and R range is (0.938-0.996). Moreover, it can be seen that ACF for selection points almost within 95% confidence intervals for the testing and training. However, it can be considered that no loss of information was observed since the most residuals of this model stayed within the confidence interval of the auto-correlation function. From the results, it can be concluded that the NN and WNN solutions can be used. Moreover, the results show that the ARXWN model can be used to predict the temperature for the Nile Delta in Egypt.

The comparison between the selected points as shown in Fig. 4, 6 and 7 shows that the linear fitting equation for ARXNN is better than ARX and ARXWN for the testing points, while ARXWN is better for training point. Table 3 presents the comparison between the training statistical points. From Table 3, it can be seen that the ARX model has the lowest RMSE (1.55°C) and R (0.943) for the Alexandria station. The worst ARX estimates belong to the Port Said station with the RMSE of 3.94°C and R of 0.599. In the case of ARXNN, the best and worst models were obtained for the Port Said (RMSE = 0.608°C) and Tanta (RMSE = 1.527°C) stations. For the ARXWN, it can be seen that the all testing points prediction were correlation with the observation temperature for all selected points. It can be obviously seen from Table 3 that the ARXWN model is better than the ARXNN in the training period.

Table 4 depicts the comparison between testing statistical points. From this table, it can be seen that the maximum and minimum RMSE took place at Damietta and Dekhila stations, respectively, for ARX model. Moreover, the best and worst case for ARXNN model are occurred at Rossetta and Belbess stations while for ARXWN are occurred at stations Khatatba and Zagazig, respectively. It can be obviously seen from Table 4 that the ARXNN and ARXWN models can be used in the testing period. But, the comparison for the ACF is shown that the ARXNN is better than ARXWN in the testing period. However, the model ARXNN is more suitable to use in our case study.

CONCLUSION

This study aims to apply the least mean square, arti cial Neural Network (NN) and Wavenet Neural network (WN) techniques for modeling long-term air temperature values by using time series observation data. In this study, the abilities of nonlinear auto-regression model with eXogeneous inputs (ARX), ARXNN and ARXWN models were investigated to predict air temperature and precipitation values using time series air temperature input-output observation data.

The data from 18 weather stations in the Nile Delta region in Egypt were used for training and testing of the introduced models. The ARX [99] least mean square, neural network and wavelet neural network models were compared with each other with respect to root-mean-squared error, determination coefficient statistics and 95% of the confidence interval for ACF. The pre-analysis observation data concluded that the maximum variance is occurred in the summer time for the monitoring stations, while low variance occurs during winter time. However, the summer time temperature change is higher than winter time. Moreover, it can be seen that the Delta main temperature changes occur for the coastal points monitoring.

The ARX model is shown lower quality in the training and testing periods. ARXWN model was found to be better than the ARXNN in the training period. In the test period, however, the ARXNN model performed better than the ARXWN model in five of nine stations. For the ARXNN and

ARXWN models, the maximum determination coefficient values were found to be 0.989 and 0.996 in Rossetta and Khatatba stations, respectively. The minimum determination coefficient values were respectively found as 0.978 and 0.938 for the ARXNN and ARXWN models in Belbess and Zagazig stations. Moreover, the 95% ACF for the residuals models shown that no loss of information was observed since the residuals of the ARXNN model stayed within the confidence interval of the auto-correlation function. It can be concluded that the ARXNN technique can be used successfully to predict the long-term monthly temperatures of any site at Nile Delta region based on previously time series temperature measurements.

ACKNOWLEDGMENTS

The authors would like to thank the collection data by Egyptian Meteorological Authority team. This work was supported by Mansoura University, Egypt.

REFERENCES

Abdelaal, M., 2012. Climatic variability of precipitation in the Egyptian coasts a study in climatology. Ph.D. Thesis, Geography Department, Faculty of Arts, Mansoura University, Egypt.

Abdelaal, M., 2014. Precipitation concentration changes in Egypt during the period (1947-2006). Proceedings of the 7th International Conference for Development and the Environment in the Arab World, March 23-25, 2014, Assuit, Egypt, pp: 403-421.

Alexandersson, H., 1986. A homogeneity test applied to precipitation data. J. Climatol., 6: 661-675.

Baigorria, G.A., E.B. Villegas, I. Trebejo, J.F. Carlos and R. Quiroza, 2004. Atmospheric transmissivity: Distribution and empirical estimation around the central andes. Int. J. Climatol., 24: 1121-1136.

CAPMS., 2014. Statistical yearbook. Arab Republic of Egypt, Central Agency for Public Mobilization and Statistics (CAPMS), Egypt.

Domroes, M. and A. El-Tantawi, 2005. Recent temporal and spatial temperature changes in Egypt. Int. J. Climatol., 25: 51-63.

El Kenawy, A., J.I. Lopez-Moreno, S.M. Vicente-Serrano and F. Morsi, 2010. Climatological modeling of monthly air temperature and precipitation in Egypt through GIS techniques. Climate Res., 42: 161-176.

El-Hussainy, F.M. and K.S.M. Essa, 1997. The phase lag of temperature behind global solar radiation over Egypt. Theor. Applied Climatol., 58: 79-86.

Frihy, O.E. and P.D. Komar, 1993. Long-term shoreline changes and the concentration of heavy minerals in beach sands of the Nile Delta, Egypt. Mar. Geol., 115: 253-261.

Ghoneim, E., J. Mashaly, D. Gamble, J. Halls and M. AbuBakr, 2015. Nile Delta exhibited a spatial reversal in the rates of shoreline retreat on the Rosetta promontory comparing pre-and post-beach protection. Geomorphology, 228: 1-14.

Kaloop, M.R., M. Sayed, D. Kim and E. Kim, 2014. Movement identification model of port container crane based on structural health monitoring system. Struct. Eng. Mech., 50: 105-119.

Kenawy, A., J.I. Lopez-Moreno, S.M. Vicente-Serrano and M. Abdelaal, 2010. Temperature variability along the Mediterranean coast and its lines to large-scale atmospheric circulation (1957-2006). Bull. Egypt. Geograph. Soc., 83: 121-140.

Kim, D.H. and I.W. Lee, 2001. Neuro-control of seismically excited steel structure through sensitivity evaluation scheme. Earthquake Eng. Struct. Dyn., 30: 1361-1377.

Kisi, O., S. Kim and J. Shiri, 2013. Estimation of dew point temperature using neuro-fuzzy and `neural network techniques. Theor. Applied Climatol., 114: 365-373.

Kisi, O. and J. Shiri, 2014. Prediction of long-term monthly air temperature using geographical inputs. Int. J. Climatol., 34: 179-186.

Kisi, O. and H. Sanikhani, 2015. Modelling long-term monthly temperatures by several data-driven methods using geographical inputs. Int. J. Climatol. 10.1002/joc.4249

Li, Q., X. Liu, H. Zhang, P. Thomas and E.R. David, 2004. Detecting and adjusting temporal inhomogeneity in Chinese mean surface air temperature data. Adv. Atmosph. Sci., 21: 260-268.

Molua, M.L., J. Benhin, J. Kabubo-Mariara, M. Ouedraogo and S. El-Marsafawy, 2010. Global climate change and vulnerability of African agriculture: Implications for resilience and sustained productive capacity. Q. J. Int. Agric., 49: 183-211.

Mpelasoka, F.S., A.B. Mullan and R.G. Heerdegen, 2001. New Zealand climate change information derived by multivariate statistical and artificial neural networks approaches. Int. J. Climatol., 21: 1415-1433.

NASA., 2015. Global climate change: Vital signs of the planet. Global Temperature, National Aeronautics and Space Administration (NASA), USA., April 2015.

NOAA., 2015. Global climate change indicators. National Climatic Data Center, National Oceanic and Atmospheric Administration (NOAA). Maryland, USA., April 2015.

Omran, M.A., 2000. Analysis of solar radiation over Egypt. Theor. Applied Climatol., 67: 225-240.

Peterson, T.C. and D.R. Easterling, 1994. Creation of homogeneous composite climatological reference series. Int. J. Climatol., 14: 671-679.

Peterson, T.C., R. Vose, R. Schmoyer and V. Razuvaev, 1998. Global historical climatology network (GHCN) quality control of monthly temperature data. Int. J. Climatol., 18: 1169-1179.

Raino, H., 1999. Homogeneity of the long-term urban data records. Atmos. Environ., 33: 3879-3883.

Sargazi, A.R., H. Badihbarzin, H. Jahantigh, M. Mahmoudi, M. Ghavidel, A.R. Sobhani and M.R. Sobhani, 2014. Assessment and forecast of yearly temperatures Using artificial neural networks and regression analysis, Case Study: Mazandaran Province, Behshahr City, Iran. Scholars J. Agric. Vet. Sci., 1: 260-264.

Sinik, N., 1992. A local climatic model of the temperature-cloudiness relationship. Theor. Applied Climatol., 46: 135-142.

Stepanek, P., 2007. AnClim-software for time series analysis (for Windows). Ph.D. Thesis, Department of Geography, Faculty of Natural Sciences, Masaryk University, Brno.

Tuomenvirta, H., 2001. Homogeneity adjustments of temperature and precipitation series-finnish and nordic data. Int. J. Climatol., 21: 495-506.

Vicente-Serrano, S.M., S. Begueria, J.I. Lopez-Moreno, M.A. Garcia-Vera and P. Stepanek, 2010. A complete daily precipitation database for northeast Spain: reconstruction, quality control and homogeneity. Int. J. Climatol., 30: 1146-1163.

WMO/TD., 2003. Guidance on metadata and homogenization. World Meteorological Organization, No. 1186, Geneva.